

# Solvatochromic properties of long alkyl chain $\pi^*$ indicators: comparison of *N,N*-dialkyl-4-nitroanilines and alkyl 4-nitrophenyl ethers

R. Helburn,<sup>1\*</sup> M. Bartoli,<sup>1</sup> K. Pohaku,<sup>1</sup> J. Maxka,<sup>2</sup> D. Compton,<sup>2</sup> B. Creedon<sup>2</sup> and C. Stimpson<sup>2</sup>

<sup>1</sup>Department of Chemistry and Physical Sciences, Pace University, 1 Pace Plaza, New York, New York 10038, USA

<sup>2</sup>Department of Chemistry, Northern Arizona University, Flagstaff, Arizona 86011, USA

Received: 18 November 2005; revised 5 July 2006; accepted 28 July 2006

**ABSTRACT:** Hydrophobic forms of the *N,N*-dialkyl-4-nitroaniline (DNAP) ( $p$ -O<sub>2</sub>NC<sub>6</sub>H<sub>4</sub>NR<sub>2</sub>) (**1a–f**) and alkyl-4-nitrophenyl ether ( $p$ -O<sub>2</sub>NC<sub>6</sub>H<sub>4</sub>OR) (**2a–c**) solvatochromic  $\pi^*$  indicators have been characterized and compared with respect to: (a) solvatochromic bandshape, (b) sensitivity expressed as  $-s$ , ( $d\bar{\nu}_{\max}/d\pi^*$ ), and (c) trends in  $-s$  with increasing length of alkyl chain(s) on the probe molecule. —Octyl 4-nitrophenyl ether ( $p$ -O<sub>2</sub>NC<sub>6</sub>H<sub>4</sub>OC<sub>8</sub>H<sub>17</sub>) (**2b**) and —decyl 4-nitrophenyl ether ( $p$ -O<sub>2</sub>NC<sub>6</sub>H<sub>4</sub>OC<sub>10</sub>H<sub>21</sub>) (**2c**) were synthesized and their solvatochromic UV/Vis absorption bands were found to maintain a Gausso-Lorentzian bandshape for the indicators in non-polar and alkyl substituted aromatic solvents, for example, hexane(s) and mesitylene. Corresponding absorption bands for **1a–f** display increasing deviation from a Gausso-Lorentzian shape in the same solvents as the alkyl chains on the indicator are increased in length all the way to C<sub>10</sub> and C<sub>12</sub>, for example, *N,N*-didecyl-4-nitroaniline ( $p$ -O<sub>2</sub>NC<sub>6</sub>H<sub>4</sub>N(C<sub>10</sub>H<sub>21</sub>)<sub>2</sub>) and *N,N*-didodecyl-4-nitroaniline ( $p$ -O<sub>2</sub>NC<sub>6</sub>H<sub>4</sub>N(C<sub>12</sub>H<sub>25</sub>)<sub>2</sub>) (**1d–f**). A plot of  $-s$  versus C<sub>n</sub> follows a 1st order decay for the DNAP indicators but is linear for the alkyl 4-nitrophenyl ethers. A discussion of how the long alkyl chains on the two types of indicators affect the orientation and overlap of  $n$  and  $\pi^*$  orbitals, and resulting solvatochromic bands is presented. For DNAP, overextending the alkyl chains to obtain greater hydrophobic character may cause the alkane component to dominate solute-solvation processes at the expense of the probe's fundamental solvatochromic character. Copyright © 2007 John Wiley & Sons, Ltd.

**KEYWORDS:** polarity; solvatochromism; indicator; solvent;  $\pi^*$

## INTRODUCTION

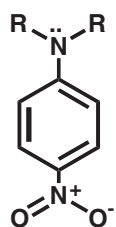
The  $\pi^*$  scale of solvent dipolarity and polarizability which is based on the UV/Vis spectral shifts of individual indicator solutes has found numerous uses since it was first introduced in 1977 by Kamlet, Abboud, and Taft.<sup>1–2</sup> Subsequent modification to scale parameters<sup>3</sup> and to the solvatochromic indicators used to produce individual dipolarity measurements,  $\pi^*$  values,<sup>4–6</sup> attest to the interest that the  $\pi^*$  scale has generated and to its overall broad utility. Among the more recent developments is the synthesis and application of indicators with increasingly long hydrophobic tails that permit the probing of solvent environments inside micelles and lipid bilayers, thus extending  $\pi^*$  measurements to these more complex organic interfacial systems for which there is considerable interest.<sup>6–11</sup> In this work, we present and compare the solvatochromic properties of two of the more hydro-

phobic forms that we have prepared. They are the long chain *N,N*-dialkyl-4-nitroanilines and some long chain alkyl 4-nitrophenyl ethers (Figs 1 and 2). These newer dyes comprise lipophilic forms of two of the seven original indicators employed by Kamlet *et al.* in their development of the original  $\pi^*$  scale.<sup>1</sup>

Of particular interest in the characterization of new polarity-sensitive indicators are (1) the shape of an individual spectral band from which the wavenumber of maximum absorption ( $\bar{\nu}_{\max}$ ) is determined and (2) the magnitude of the slope of a linear plot of  $\bar{\nu}_{\max}$  versus solvent  $\pi^*$ , the  $-s$  parameter.<sup>1</sup> Deviation from a Gaussian or Lorentzian band shape can result in a lack of accuracy and precision in locating  $\bar{\nu}_{\max}$  and in certain cases may invalidate the use of the indicator as a polarity probe.  $-s$  provides a measure of an indicator's sensitivity, for example, spectral shifting capability. Larger values (of  $-s$ ) result in a greater ability of the probe to resolve small differences in dipolarity among solvation environments. For heterogeneous systems where the probe resides in an anisotropic environment, such differences can be significant. Optimization of these two properties is thus a

\*Correspondence to: R. Helburn, Department of Chemistry and Physical Sciences, Pace University, 1 Pace Plaza, New York, NY 10038, USA.

E-mail: rhelburn@fsmail.pace.edu



R= alkyl groups, each with same no. of carbons (n); n= 1 (**1a**), 2 (**1b**), 3 (**1c**), 8 (**1d**), 10 (**1e**), 12 (**1f**).

**Figure 1.** Homologous series of di-*n*-(alkyl)-4-nitroaniline (DNAP) indicators: *N,N*-dimethyl-4-nitroaniline (**1a**), *N,N*-diethyl-4-nitroaniline (**1b**), *N,N*-dipropyl-4-nitroaniline (**1c**), *N,N*-dioctyl-4-nitroaniline (**1d**), *N,N*-didecyl-4-nitroaniline (**1e**), *N,N*-didodecyl-4-nitroaniline (**1f**)

consideration in tailoring new  $\pi^*$  indicators for use in these complex systems.

## Theory and background

Solvatochromic dyes act as indicators of solvent polarity by exhibiting shifts in the positions of their UV/Vis absorption bands. The 'push-pull' molecular system illustrated in Fig. 3 shows the structural features that give solvatochromic dyes their unique spectroscopic properties. The  $\pi^*$  indicators are a class of solvatochromic dyes that respond to the non-specific portion of van der Waal's forces, for example, solvent induction, dispersion, and dipolar effects,<sup>1-2</sup> where the  $\pi^*$  parameter is calculated from the positions of UV/Vis absorption bands of an indicator in the solvent environment of interest. Experimental values (of  $\pi^*$ ) are related to the transition energy through a linear solvation energy relationship (LSER) of the following form.

$$\bar{\nu}_{\max} = \bar{\nu}_0 + s\pi^* \quad (1)$$

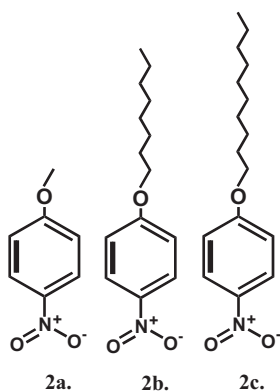


**Figure 2.** Homologous series of solvatochromic 4-alkyloxynitrobenzenes: 4-nitroanisole (**2a**), 4-octyloxynitrobenzene (**2b**), and 4-decyloxynitrobenzene (**2c**)

In Equation 1,  $\bar{\nu}_{\max}$  is the wavenumber of maximum absorption, in  $\text{cm}^{-1}$ , for the indicator in the solvent of interest;  $\bar{\nu}_0$  is the wavenumber of maximum absorption for the indicator in cyclohexane. Within the context of the  $\pi^*$  scale, the slope  $s$  (Eqn 1) reflects the magnitude of spectral shift over a range of solvents that span two reference points, cyclohexane ( $\pi^* = 0.00$ ) and dimethylsulfoxide ( $\pi^* = 1.00$ ).<sup>1</sup> A correction term ( $d\delta$ ) that weighs the relative polarizability of individual solvents according to membership in one of three structural classes, for example, chlorinated ( $d\delta = 0.5$ ), aliphatic ( $d\delta = 0.0$ ), or aromatic ( $d\delta = 1.00$ ) solvents, was added to the LSER (Eqn 1) in 1981<sup>3</sup> though the parameter has not been consistently applied.

The first  $\pi^*$  scale<sup>1</sup> was based on the UV/Vis spectra of seven indicators where the intent was to create an approach that combined the individual spectral anomalies of a suite of probes.<sup>1</sup> It was later suggested that such averaging of spectral information blurred meaningful contributions and that a scale based on the UV/Vis absorption bands of a single indicator was to be preferred.<sup>2</sup> Of the seven initial probes, the *N,N*-dialkyl-4-nitroanilines, **1a** and **1b**, were found to be most sensitive to non-specific solvent interactions (e.g., high  $-s$ , Eqn 1). However, **1b** was reported to have a significant solvent-dependent bandshape suggesting that longer-chain versions of this indicator might suffer similarly. 4-Nitroanisole (**2a**), while less sensitive, that is, lower  $-s$ , was considered to be most desirable based on its Gausso-Lorentzian bandshape which was seen to be constant for media ranging all the way from the gas phase to the most polar solvents.<sup>2,12</sup> As we have prepared long alkyl chain versions of both **1a–b** and **2a** (Figs 1 and 2),<sup>13,14</sup> we can now pursue a more rigorous comparison of the solvatochromic and spectral band shape properties of these more hydrophobic  $\pi^*$  indicators.

## EXPERIMENTAL

### Reagents (solvents)

Acetonitrile (99.9% anhydrous), benzonitrile (99+% spectrophotometric grade), cyclohexane (99+% spectrophotometric grade), hexanes and *n*-hexane (spectrophotometric grade), *n*-heptane (spectrophotometric grade), *n*-pentane (99+% spectrophotometric grade), 1,4-dioxane (99.0% spectrophotometric grade), *N,N*-dimethylacetamide (99+% spectrophotometric grade), *N,N*-dimethylformamide (DMF) (99.8% anhydrous), dimethylsulfoxide (DMSO) (99.7% anhydrous), chlorobenzene (99+% spectrophotometric grade), benzene (99+% spectrophotometric grade), toluene (99.8% anhydrous), mesitylene (99%), *n*-butyl acetate (spectrophotometric grade), ethyl acetate (99.9% spectrophotometric grade), diethyl ether (anhydrous), di-*n*-butyl ether (99+%), di-*n*-propyl ether (99% anhydrous), tetrahydrofuran

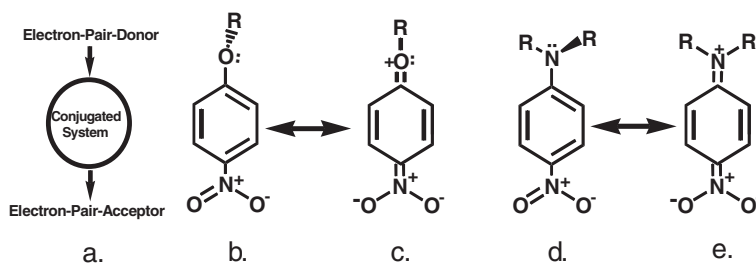


**Figure 3.** Model of a solvatochromic  $\pi^*$  indicator (a); dipolar mesomeric structures of alkyl-4-nitrophenyl ethers in the ground (b) and excited (c) state; dipolar mesomeric structures of DNAP indicators in the ground (d) and excited (e) state

(THF) (99.5% anhydrous), pyridine (99.8% anhydrous), *N*-methylpyrrolidin-2-one (NMP), 1,2-dichloroethane (extra dry), tetrachloroethene (99+% spectrophotometric grade), and triethylamine (99.7%) were purchased from Acros and used as received.

### Instrumentation

UV/Vis spectra were recorded on both Varian Cary 3E and Beckman DU-640 scanning dispersive UV/Vis spectrophotometers. Values for spectral bandwidth were 1.2 and 1.8 nm, respectively. Spectral data collection intervals were 0.4 and 0.5 nm, respectively. For the Cary 3E, the cell block was thermostatted to 25 °C. Ambient room temperatures were used in the operation of the Beckman DU-640. All spectra were digitized and converted to an ASCII format and imported into a Quattro Pro or Excel spreadsheet for background correction and subsequent data analysis.

<sup>1</sup>H NMR spectra, obtained for structure confirmation on the synthesized alkyl 4-nitrophenyl ethers, were measured at 400 MHz on Gemini Varian FT-NMR instrumentation. Chemical shifts were referenced to tetramethylsilane (TMS). CDCl<sub>3</sub> was used as the supporting solvent in all NMR measurements. Separations for synthesis reaction mixtures were carried out using thin-layer chromatography (TLC) and gas chromatography with mass spectrometric detection (GC/MS). Diagnostic TLC was performed using Whatman 250  $\mu$ m silica gel plates. GC/MS data were collected on an HP Model 5890 chromatograph with an HP Model 5971 mass selective

detector. Molecular masses were taken from the mass spectral data.

### Synthesis

An homologous suite of *N,N*-dialkyl-4-nitroanilines was synthesized using methods described in Mansour *et al.*<sup>5</sup> Indicators in this group that were characterized for the present study are the crystalline *N,N*-dipropyl-4-nitroaniline, *N,N*-dioctyl-4-nitroaniline, *N,N*-didecyl-4-nitroaniline, and *N,N*-didodecyl-4-nitroaniline. 4-Alkylloxynitrobenzenes with alkyl chain lengths of two, four, six, seven, eight, and ten carbons were synthesized as follows.

**Procedure for synthesis of alkyl 4-nitrophenyl ethers (R—O—Ph—NO<sub>2</sub>).** In a 3-necked 250-mL round-bottomed flask equipped with a dropping funnel and reflux condenser, approximately 0.02 mole of 4-nitrophenol was added with approximately 0.02 mole of K<sub>2</sub>CO<sub>3</sub> in 40 mL of acetone. The acetone solution was brought to reflux and neat haloalkanes were added slowly. The reaction was followed by TLC until completion about 48–72 h, depending on alkyl chain length. After cooling, the acetone was removed in a rotary evaporator. The solid was dissolved in 30 mL of distilled water and extracted with three 30 mL portions of *tert*-butyl methyl ether. The ether solution was washed with three 30 mL portions of 3 M aqueous NaOH solution until the yellow color of the phenolate anion was no longer present. The ether was dried and then removed by rotary evaporation. The materials are low melting solids. No melting points were recorded. Purity was checked by GC/MS and NMR. The yields were not optimized (Table 1).<sup>15</sup>

**Table 1.** Summary of procedure for synthesis of **2b–c** and additional species

R-	K <sub>2</sub> CO <sub>3</sub> mmol (g)	4-nitrophenol mmol (g)	R-X mmol (g)	Reflux time (h)	R—O—Ph—NO <sub>2</sub> (g) % yield
-Butyl <sup>b</sup>	17.03 (2.34)	16.84 (2.343)	Iodobutane 16.90 (3.11)	48	(2.36) 71%
-Hexyl	19.58 (2.70)	20.23 (2.814)	Iodoheptane 18.30 (4.13)	57	(1.86) 43%
-Heptyl <sup>b</sup>	18.59 (2.57)	19.18 (2.669)	Iodoheptane 18.30 (4.13)	64	(2.58) 63%
-Octyl <sup>a</sup>	18.86 (2.60)	18.07 (2.516)	Iodoheptane 18.30 (4.13)	70	(2.90) 69%
-Decyl <sup>a</sup>	18.50 (2.55)	18.999 (2.643)	Iododecane 18.35 (4.92)	71	(3.34) 61%

<sup>a</sup> Long alkyl chain dyes used in spectral studies and comprehensive  $\pi$ - $\pi^*$  determinations.

<sup>b</sup> Used to corroborate observed trends in  $\pi$ - $\pi^*$ .

**Identification of the alkyl 4-nitrophenyl ethers (R—O—Ph—NO<sub>2</sub>).** *Butyl 4-nitrophenyl ether* (CAS 7244-78-2). <sup>1</sup>H NMR (CDCl<sub>3</sub>) δ 0.98 (t 3H, CH<sub>3</sub>), 1.5 (m 2H, CH<sub>2</sub>), 1.8 (m 2H, CH<sub>2</sub>), 4.05 (t 2H, CH<sub>2</sub>), 6.93 (d 2H, Ar), 8.16 (d 2H, Ar); GC/MS *m/z* 195, calcd *m/z* for C<sub>10</sub>H<sub>13</sub>NO<sub>3</sub> 195.

*Hexyl 4-nitrophenyl ether* (CAS 15440-98-9). <sup>1</sup>H NMR (CDCl<sub>3</sub>) δ 0.89 (t 3H, CH<sub>3</sub>), 1.33 (m 6H CH<sub>2</sub>), 1.45 (m 2H, CH<sub>2</sub>), 1.81 (m 2H, CH<sub>2</sub>), 4.03 (t 2H, CH<sub>2</sub>), 6.91 (d 2H, Ar), 8.15 (d 2H, Ar); GC/MS *m/z* 223, calcd *m/z* for C<sub>12</sub>H<sub>15</sub>NO<sub>3</sub> 223.

*Heptyl 4-nitrophenyl ether* (CAS 13565-36-1). <sup>1</sup>H NMR (CDCl<sub>3</sub>) δ 0.89 (t 3H, CH<sub>3</sub>), 1.32 (m 6H CH<sub>2</sub>), 1.45 (m 2H, CH<sub>2</sub>), 1.81 (m 2H, CH<sub>2</sub>), 4.03 (t 2H, CH<sub>2</sub>), 6.91 (d 2H, Ar), 8.15 (d 2H, Ar); GC/MS *m/z* 237, calcd *m/z* for C<sub>13</sub>H<sub>19</sub>NO<sub>3</sub> 237.

*Octyl 4-nitrophenyl ether* (CAS 49562-76-7). <sup>1</sup>H NMR (CDCl<sub>3</sub>) δ 0.88 (t 3H, CH<sub>3</sub>), 1.31 (m 8H, CH<sub>2</sub>), 1.46 (m 2H, CH<sub>2</sub>), 1.81 (m 2H, CH<sub>2</sub>), 4.04 (t 2H, CH<sub>2</sub>), 6.93 (d 2H, Ar), 8.19 (d 2H, Ar); GC/MS *m/z* 251, calcd *m/z* for C<sub>14</sub>H<sub>21</sub>NO<sub>3</sub> 251.

*Decyl 4-nitrophenyl ether* (CAS 31657-37-1). <sup>1</sup>H NMR (CDCl<sub>3</sub>) δ 0.84 (t 3H, CH<sub>3</sub>), 1.27 (m 12H, CH<sub>2</sub>), 1.41 (m

2H, CH<sub>2</sub>), 1.78 (m 2H, CH<sub>2</sub>), 3.98 (t 2H, CH<sub>2</sub>), 6.87 (d 2H, Ar), 8.09 (d 2H, Ar); GC/MS *m/z* 279, calcd *m/z* for C<sub>16</sub>H<sub>25</sub>NO<sub>3</sub> 279.

### Determination of *s* and bandshape studies

Values of *s* were calculated for each new indicator from their individual UV/Vis spectra in 20–23 non-hydrogen-bond-donor (non-HBD) solvents. The solvents (Tables 2–4) were selected from a list of non-HBD and non-hydrogen-bond-acceptor (non-HBA) solvents utilized by Kamlet *et al.*<sup>1</sup> in the construction of their original  $\pi^*$  scale and in the estimation of *s* for several of their original small molecule indicators.<sup>1</sup> Values of  $\bar{\nu}_{\max}$  were determined from the 90% method<sup>16</sup> and from the best fit Gaussian or Lorentzian as applied to the top 0.1 to 0.15 absorbance range of an individual band; note: our preliminary studies showed that fitting of the entire spectral band yields  $\lambda_{\max}$  values that are affected by the adjacent baseline.<sup>13</sup> The ‘goodness’ of the fit, for example, Gaussian or Lorentzian, is expressed via Chi-square and *r*<sup>2</sup> values, obtained from the individual fitting routines. Model fitting was implemented using *Origin* ver. 6.1 software. In addition to providing  $\bar{\nu}_{\max}$  values, Gaussian and Lorentzian fitting of individual spectra was used to compare bandshapes for C<sub>8</sub> and C<sub>10</sub>

**Table 2.** Values of  $\bar{\nu}_{\max}$  in cm<sup>-1</sup> for *N,N*-dipropyl-4-NO<sub>2</sub> (1) and *N,N*-dioctyl-4-NO<sub>2</sub> (2)

	Solvent	(1)			(2)		
		Gaussian <sup>a</sup>	Lorentzian <sup>b</sup>	90/90	Gaussian <sup>c</sup>	Lorentzian <sup>d</sup>	90/90
1	Benzonitrile	24.767	24.765	24.69	24.625	24.624	24.61
2	Chlorobenzene	25.385	25.384	25.32	25.279	25.279	25.27
3	<i>n</i> -Heptane	27.543	27.543	27.55	27.369	27.369	27.35
4	<i>N,N</i> -Dimethylacetamide	24.709	24.707	24.7	24.707	24.707	24.7
5	DMF	24.662	24.660	24.66			
6	DMSO	24.309	24.307	24.32	24.223	24.222	24.2
7	Benzene	25.853	25.851	25.71	25.783	25.781	25.73
8	<i>n</i> -Butyl acetate	25.978	25.976	25.91	25.867	25.867	25.81
9	Butyl ether	26.829	26.828	26.72	26.693	26.692	26.65
10	Di-isopropyl ether	26.793	26.792	26.72	26.653	26.645	26.62
11	THF	25.669	25.669	25.65	25.581	25.581	25.58
12	Pyridine	24.767	24.765	24.77	24.702	24.700	24.69
13	NMP	24.590	24.588	24.58	24.521	24.520	24.5
14	1,2-Dichloroethane	24.963	24.962	24.95	24.828	24.828	24.82
15	Triethylamine	27.070	27.070	27.06	26.910	26.911	27.03
16	Tetrachloroethene	26.661	26.660	26.63	26.535	26.534	26.49
17	1,4-Dioxane	25.818	25.817	25.78	25.718	25.716	25.74
18	Ethyl ether	26.621	26.621	26.58	26.388	26.386	26.38
19	<i>n</i> -Hexane	27.373	27.373	27.38	27.209 <sup>e</sup>	27.210 <sup>e</sup>	27.18 <sup>e</sup>
20	<i>n</i> -Pentane	27.719	27.718	27.68			
21	Acetonitrile	24.908	24.885	24.89			
22	Mesitylene	26.231	26.230	26.24	26.227	26.231	26.24
23	Ethyl acetate				25.740	25.740	25.71

<sup>a</sup> Range of Chi-square =  $9.5 \times 10^{-6}$  to  $4.0 \times 10^{-5}$ ; range of *r*<sup>2</sup> = 0.9539 to 0.9886.

<sup>b</sup> Range of Chi-square =  $9.3 \times 10^{-6}$  to  $4.0 \times 10^{-5}$ ; range of *r*<sup>2</sup> = 0.9489 to 0.9893.

<sup>c</sup> Range of Chi-square =  $7.10 \times 10^{-6}$  to  $5.0 \times 10^{-5}$ ; range of *r*<sup>2</sup> = 0.9037 to 0.9923.

<sup>d</sup> Range of Chi-square =  $7.15 \times 10^{-6}$  to  $6.0 \times 10^{-5}$ ; range of *r*<sup>2</sup> = 0.9152 to 0.9919.

<sup>e</sup> Values are for cyclohexane.

**Table 3.** Values of  $\bar{\nu}_{\max}$  in  $\text{cm}^{-1}$  for *N,N*-didecyl-4-NO<sub>2</sub> (1) and *N,N*-didodecyl-4-NO<sub>2</sub> (2)

	Solvent	(1)			(2)		
		Gaussian <sup>a</sup>	Lorentzian <sup>b</sup>	90/90	Gaussian <sup>c</sup>	Lorentzian <sup>d</sup>	90/90
1	Acetone	25.073	25.073	25.14	25.080	25.078	25.06
2	Benzonitrile	24.597	24.596	24.58	24.624	24.615	24.62
3	Chlorobenzene	25.272	25.272	25.25	25.290	25.290	25.29
4	<i>n</i> -Heptane	27.359	27.359	27.33	27.354	27.354	27.34
5	<i>n</i> -Hexane	27.199	27.199	27.21	27.196 <sup>e</sup>	27.196 <sup>e</sup>	27.26 <sup>e</sup>
6	<i>N,N</i> -Dimethylacetamide	24.617	24.616	24.61	24.642	24.640	24.66
7	DMF	24.551	24.548	24.54	24.554	24.553	24.55
8	DMSO	24.204	24.203	24.2	24.199	24.198	24.2
9	Benzene	25.813	25.811	25.63	25.825	25.823	25.82
10	Toluene	26.008	26.006	25.98	25.992	25.997	26.028
11	<i>n</i> -Butyl acetate	25.871	25.870	25.87	25.859	25.823	25.85
12	Ethyl acetate	25.717	25.716	25.73	25.730	25.997	25.72
13	di-ethyl ether	26.454	26.453	26.46			
14	di-butyl ether	26.670	26.670	26.64	26.715	26.714	26.64
15	di-2-propyl ether	26.651	26.649	26.62	25.720 <sup>f</sup>	25.720 <sup>f</sup>	25.71 <sup>f</sup>
16	THF	25.574	25.573	25.54	25.590	24.628	25.55
17	Pyridine	24.679	24.679	24.67	24.629	24.494	24.67
18	NMP	24.474	24.478	24.45	24.496	24.494	24.5
19	1,2-Dichloroethane	24.844	24.844	24.83	24.871	24.876	24.85
20	Triethylamine	26.866	26.866	27.01	26.930	26.931	26.92
21	Tetrachloroethene	26.524	26.525	26.50	26.570	26.571	26.5
22	Mesitylene				26.254	26.252	26.25

<sup>a</sup> Range of Chi-square =  $9.5 \times 10^{-6}$  to  $4.0 \times 10^{-5}$ ; range of  $r^2 = 0.9539$  to  $0.9886$ .

<sup>b</sup> Range of Chi-square =  $9.3 \times 10^{-6}$  to  $4.5 \times 10^{-5}$ ; range of  $r^2 = 0.9489$  to  $0.9893$ .

<sup>c</sup> Range of Chi-square =  $7.10 \times 10^{-6}$  to  $5.0 \times 10^{-5}$ ; range of  $r^2 = 0.9037$  to  $0.9923$ .

<sup>d</sup> Range of Chi-square =  $7.15 \times 10^{-6}$  to  $6.0 \times 10^{-5}$ ; Range of  $r^2 = 0.9152$  to  $0.9919$ .

<sup>e</sup> Values are for cyclohexane.

<sup>f</sup> Values are for the cyclic ether dioxane.

4-alkyloxynitrobenzenes with those of the C<sub>3</sub>, C<sub>8</sub>, C<sub>10</sub>, and C<sub>12</sub> DNAP indicators.

## RESULTS AND DISCUSSION

### Solvents and solvatochromic absorption bands

The ranges of  $\lambda_{\max}$  for solvatochromic bands of the DNAP indicators (Fig. 1) versus those of the alkyl 4-nitrophenyl ethers (Fig. 2) in non-HBD solvents of varying dipolarity (Tables 2–4) are 350–424 nm and 292–319 nm, respectively. The more blue-shifted range of  $\lambda_{\max}$  for the alkyl nitrophenyl ethers resulted in our excluding acetone and other ketones from the solvent list for these indicators since UV absorption by those solvents overlapped strongly with the solvatochromic absorption bands of **2b** and **2c**, which accordingly could not be resolved. Spectra of other conjugated solvents such as benzene, toluene, mesitylene, and NMP overlap partially with solvatochromic bands of the long chain alkyloxy dyes such that bands for these indicators could be resolved when the solvent spectrum was subtracted from that of the solution; thus these latter solvents were included in the list of those used in establishing LSERs

(Eqn 1) for **2b** and **2c** (Table 4). We note that the spectrum of pyridine overlaps too strongly with the solvatochromic band of **2a** in that solvent while **2b** and **2c** have solvatochromic bands that are slightly red shifted when in pyridine such that this solvent is usable for establishing  $\pi^*$  scales based on the longer-chain alkyloxy dye.

Values of  $\bar{\nu}_{\max}$  obtained via the three methods, Gaussian and Lorentzian fit, and the 90% method of Kamlet *et al.*,<sup>16</sup> from individual UV/Vis spectra of the *N,N*-dipropyl, dioctyl, didecyl, and didodecyl-4-nitroanilines in each of 20–23 solvents are given in Tables 2–3. Corresponding  $\bar{\nu}_{\max}$  values for the C<sub>8</sub> and C<sub>10</sub> alkyl 4-nitrophenyl ethers are listed in Table 4. Use of both Gaussian and Lorentzian spectral band fitting as a means for locating and estimating  $\lambda_{\max}$  for bands of these two types of  $\pi^*$  indicators has permitted us to simultaneously examine band shape in a statistical manner, for example, as the extent of deviation from a Gaussian or Lorentzian bandshape or by comparing  $\lambda_{\max}$  from the individual routines. For example, solvatochromic bands of the DNAP indicators in all solvents showed differences in magnitude of fitted  $\lambda_{\max}$ , between individual Gaussian and Lorentzian fit, that ranged from 0 to 0.37 nm. The differences between the two approaches were not more than 0.03 nm for bands of the C<sub>8</sub> and C<sub>10</sub> alkyl 4-nitrophenyl ethers. The errors in individual

**Table 4.** Values of  $\bar{\nu}_{\max}$  in  $\text{cm}^{-1}$  for 4-octyloxynitrobenzene (1) and 4-decyloxynitrobenzene (2)

#	Solvent	(1)		(2)	
		Gaussian <sup>a</sup>	Lorentzian <sup>b</sup>	Gaussian <sup>c</sup>	Lorentzian <sup>d</sup>
1	Acetonitrile	32.287	32.287	32.184	32.184
2	Benzonitrile	31.760	31.758	31.706	31.706
3	Chlorobenzene	32.220	32.219	32.201	32.501
4	Cyclohexane	33.790	33.789	34.071	34.069
5	<i>n</i> -Heptane	33.931	33.930	33.940	33.939
6	<i>N,N</i> -Dimethylacetamide	31.809	31.809	31.820	31.819
7	DMF	31.800	31.930	31.774	31.773
8	DMSO	31.323	31.323	31.480	31.478
9	Benzene	32.521	32.521	32.503	31.501
10	Mesitylene	32.886	32.883	32.753	32.752
11	Ethyl acetate	32.751	32.751	32.818	32.817
12	di-ethyl ether	33.298	33.296	33.283	33.283
13	di-butyl ether	33.364	33.363	33.367	33.367
14	THF	32.510	32.510	33.155	33.153
15	Pyridine	31.735	31.736	31.709	31.707
16	NMP	31.560	31.560	31.576	31.576
17	1,2-Dichloroethane	31.815	31.814	31.984	31.983
18	Triethylamine	33.667	33.666	33.765	33.764
19	Tetrachloroethene	33.184	33.184	33.135	33.136
20	Dioxane	32.599	32.598	32.639	32.639
21	Pentane			34.211	34.214
22	di-2-propyl ether	33.35	33.46	33.374	33.374
23	Toluene	32.61	32.59	32.592	32.592

<sup>a</sup> Range of Chi-square =  $1.85 \times 10^{-6}$  to  $2.0 \times 10^{-5}$ ; single outliers at  $1.8 \times 10^{-4}$  and  $3.8 \times 10^{-4}$  for benzonitrile and triethylamine, respectively; range of  $r^2 = 0.9745$  to  $0.9982$ .

<sup>b</sup> Range of Chi-square =  $2.02 \times 10^{-6}$  to  $2.0 \times 10^{-5}$ ; single outliers at  $1.9 \times 10^{-4}$  and  $3.9 \times 10^{-4}$  for benzonitrile and triethylamine, respectively; range of  $r^2 = 0.9739$  to  $0.9980$ .

<sup>c</sup> Range of Chi-square =  $7.78 \times 10^{-7}$  to  $1.0 \times 10^{-5}$ ; range of  $r^2 = 0.9767$  to  $0.9986$ .

<sup>d</sup> Range of Chi-square =  $1.37 \times 10^{-6}$  to  $2.0 \times 10^{-5}$ ; range of  $r^2 = 0.9870$  to  $0.9985$ .

spectral fitting routines expressed as Chi-square (*note*: the larger the Chi-square value, the poorer the fit) and  $r^2$  are also relevant. For example, the average Chi-square value for individual Gaussian fits over the range of solvents was 36 times greater for **1e** (*N,N*-didecyl-4-nitroaniline) than for the single chain 4-decyloxynitrobenzene (**2c**). Looking at the corresponding  $r^2$ , we see that 90% of the  $r^2$  values were 0.99 or greater for **2c**, whereas for **1e** only 5% of those values were greater than 0.99. A very similar result was obtained for the Lorentzian fits where average Chi-square values for fitting solvatochromic bands of *N,N*-didecyl-4-nitroaniline (**1e**) were 28 times greater than those of **2c** (4-decyloxynitrobenzene) with 90% of  $r^2$  greater than 0.99 for the latter alkyloxy dye and just 5% of  $r^2$  greater than 0.99 for the *N,N*-didecyl-4-nitroaniline.

The implications of these fitting data (e.g., summaries of  $r^2$  and Chi-square for Gaussian and Lorentzian fits) are illustrated in Figs 4 and 5. Figure 4 shows that both solvatochromic bands of **2c** and its short alkyl chain counterpart **2a** in the non-polar solvent hexanes maintain a Gausso-Lorentzian bandshape. Likewise, the solvatochromic band for **1e** in hexanes deviates in shape from that of **1a**, presenting an overall *less* 'Gaussian-like' band. Laurence *et al.* (1994)<sup>2</sup> have stated that of all the smaller molecule solvatochromic  $\pi^*$  indicators, **1a** and **2a** are among the choice molecular probes based on their

constant Gausso-Lorentzian bandshape which is maintained over a wide range of solvent polarities, but that lengthening the alkyl chain on **1a** to two carbons, for example, **1b**, results in severe bandshape distortions in spectra of **1b**, especially for the most non-polar alkane solvent environments. Unlike that of the DNAP indicators (Fig. 5), we observe that long alkyl chain versions of 4-nitroanisole, **2a**, do not exhibit such spectral bandshape deviations (Fig. 4).

In the earlier studies of indicator-specific spectral anomalies,<sup>12</sup> it was further suggested that polarizable

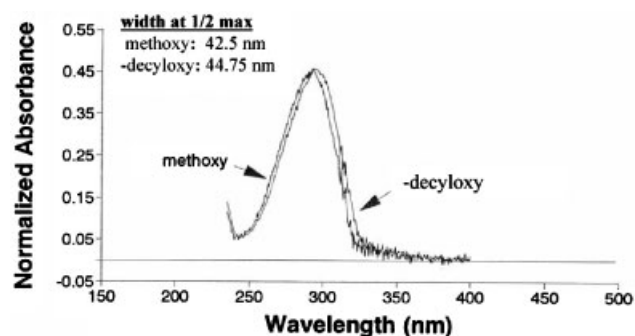


**Figure 4.** Solvatochromic (UV/Vis) absorption bands of **2a** (left) and **2c** (right) in hexane(s)

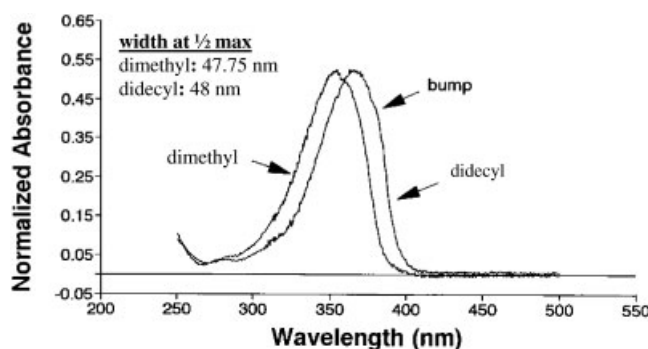


**Figure 5.** Solvatochromic (UV/Vis) absorption bands for **1a** and **1e** in hexane(s)

solvents such as toluene, *p*-xylene, and mesitylene could also influence the vibrational fine structure and bandshape for solvatochromic bands of **1b**.<sup>12</sup> In this work, we find that such effects, while somewhat evident in spectra of **1b**, for mesitylene, become much further exaggerated in spectra of **1d–e** in that solvent. Fig. 6 illustrates the progressive increase in deviation from a Gausso-Lorentzian bandshape as the alkyl chains are increased in length (**1a–d**) for selected DNAP indicators in mesitylene. The first appearance of spectral broadening

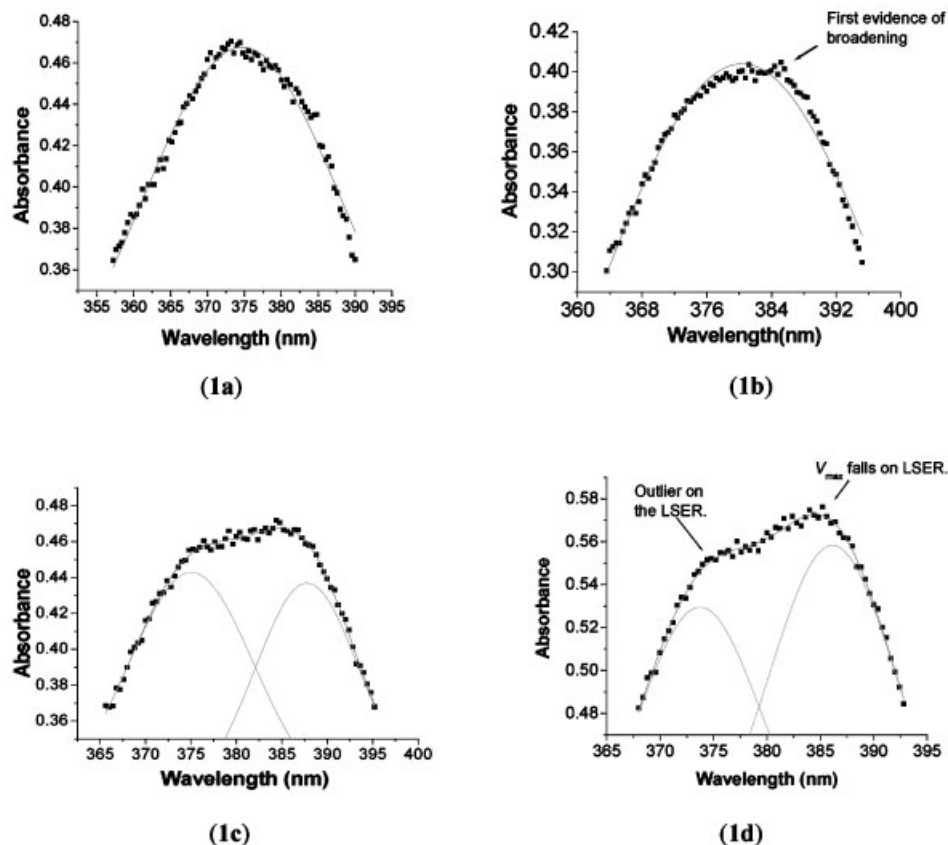


**Figure 6.** UV/Vis spectra of the upper portions of individual solvatochromic absorption bands (.....) with best fit single or double peak Gaussian fit (—) for **1a–d** in mesitylene. For Gaussian dual peak fit of **1d** (*N,N*-dioctyl-4-nitroaniline):  $\lambda_{\max}$  (1) = 373.7 nm (outlier on LSER for **1d**),  $\lambda_{\max}$  (2) = 386.1 nm (point lies on the LSER for **1d**; note: for single peak Gaussian fit of spectrum **d**,  $\lambda_{\max}$  = 381.2 nm

is highlighted for **1b** (Fig. 6–1b) where these results are consistent with previous findings.<sup>12</sup> The distortion becomes increasingly exaggerated for **1c** and **1d** such that a dual peak spectral fitting routine, as opposed to a single Gaussian or Lorentzian, more accurately describes the solvatochromic band. Values of  $r^2$  and Chi-square for the dual peak fit of the band(s) of **1d** are 0.99 and  $4.6 \times 10^{-6}$ , respectively. Conversely, the spectrum of **2b**, the corresponding alkyloxy indicator, in mesitylene (Fig. 7) shows that the long chain alkyl 4-nitrophenyl ethers are not similarly affected; the solvatochromic band for **2b**, 4-octyloxynitrobenzene, in mesitylene shows no such spectral distortion;  $r^2 = 0.98$ , Chi-square =  $5.8 \times 10^{-6}$  for the single peak Gaussian fitted band.

### Spectral effects and electron-pair-donor groups

Earlier discussions of the effect(s) of different electron-pair-donor groups on the UV/Vis spectroscopic properties of  $\pi^*$  indicators have almost always invoked steric attributes on the part of the donor substituent to explain their differing effect on the solvatochromic properties of the probe.<sup>1</sup> In particular, it has been stated in the context

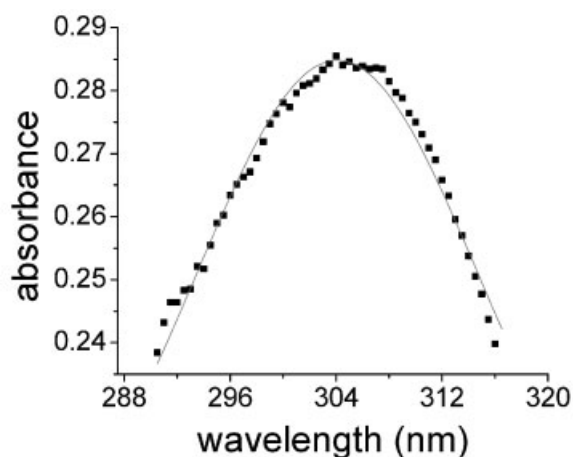


**Figure 7.** UV/vis spectrum of upper portion of solvatochromic absorption band (.....) with best fit Gaussian (\_\_\_\_) of **2b** in mesitylene

of *n*-alkyl groups that depending on structure, the donor substituent can sterically hinder solvation of the non-bonding (*n*) electron pair. This in turn affects intramolecular charge transfer and the resulting dipolar properties of the indicator in response to the solvent (Fig. 3c and e). For small short-alkyl chain donor substituents, the steric hindrance argument would seem reasonable. But if a particular spectroscopic effect, for example, bandshape distortion, becomes increasingly pronounced as the alkyl chains are extended beyond that which could be expected to provide simple steric blocking of the lone electron-pair, then another mechanism might be proposed. The two vibrationally separated absorption bands (Fig. 6-1d) seen in spectra of *N,N*-dioctyl-4-nitroaniline in mesitylene which are less pronounced for the *N,N*-dipropyl (**1c**; Fig. 6-1c) and barely existent for *N,N*-diethyl-4-nitroaniline (**1b**; Fig. 6-1b) are examples of this situation. We suggest that motions of the longer alkyl chains on the donor group affect the conformation of the indicator and the orientation of the lone electron pair in relation to the solvent and to the  $\pi^*$  orbital with which it overlaps during a transition (*n*- $\pi^*$ ). Moreover, it is not inconceivable that the very long alkyl chains affect the nature of the solvent in the vicinity of the *n* orbital, for these indicators. This latter effect is easy to envision in the case of *N,N*-didecyl-4-nitroaniline (**1e**) and *N,N*-didodecyl-4-nitroaniline (**1f**) as the alkyl moieties of these dyes are so long that they actually become part of the solvent in the *n* orbital region of the molecule.

That these spectral effects are seen primarily in pure alkane solvents and in alkane substituted benzenes, both of which have structural motifs in common with DNAP indicators, suggest the existence of non-specific solute-solvent interactions that are most pronounced for these solvent-dye systems. Where the *n* orbital of the DNAP indicator is not directly oriented toward the solvent as

compared to that of the alkyloxy dye, the result due to motions of the alkyl chain pair is an uneven ability of the (*n*) orbital to overlap directly with the neighboring  $\pi^*$  orbital (Fig. 3e) resulting in two conformationally distinct excited states, one that is less well relaxed (band at  $\lambda_{\max} = 373.7$  nm, Fig. 6-1d) and one that is more stable (band at  $\lambda_{\max} = 386.1$  nm, Fig. 6-1d), that is, based on orientation of the *n* orbital with respect to the  $\pi^*$  orbital. We suggest that the longer-wavelength lower-energy absorption ( $\lambda_{\max} = 386.1$  nm, Fig. 6-1d) is the useful solvatochromic band as  $\bar{\nu}_{\max}$  for this latter peak falls neatly on the line of a linear plot of  $\bar{\nu}_{\max}$  versus  $\pi^*$  while  $\bar{\nu}_{\max}$  for the less stable excited state ( $\lambda_{\max} = 373.7$  nm, Fig. 6d), which varies slightly more with alkyl chain length than the longer wavelength band, exists as an outlier on the LSER for that indicator. For *N,N*-diethyl-4-nitroaniline (**1b**), this conformational effect is not well pronounced resulting in an *apparent*  $\lambda_{\max}$  for the solvatochromic band that is closer to an average of these effects (Fig. 6-1b,  $\lambda_{\max} = 381.2$  nm).

The *n* orbital on the corresponding long chain 4-alkyloxynitrobenzene is oriented more directly toward the solvent over a wide range of O-alkyl chain lengths. Motions on the part of the single alkyl chain on these nitrophenyl ether probes do not affect solvation of the *n* electrons on the oxygen of this indicator or their orientation with respect to the neighboring  $\pi^*$  orbital on the excited-state resonance structure (see Fig. 3c). Thus, no such conformational spectral effects are seen for the probe in mesitylene (Fig. 7) or any other solvent.

### LSERS and trends in $-s$

LSERs (Eqn 1) were prepared for **1c-f** and **2b-c** using the values of  $\bar{\nu}_{\max}$  listed in Tables 2-4, in order to rigorously determine  $-s$  for the probes and to observe trends in  $-s$  over the range of alkyl chain lengths for these two types of  $\pi^*$  indicators (Figs 1 and 2). For consistency in comparison of values, we have re-determined  $-s$  for the well characterized small molecule probes (**1a-b** and **2a**) using the same solvent list (Tables 2-4); these values compare favorably with those of Kamlet *et al.*<sup>1</sup> Table 5 summarizes all  $-s$  values for indicators in this work computed to date, including some previously published seven-point determinations.<sup>4,8</sup>

We suggest that the conformational effects proposed for **1e-f** in the solvent mesitylene, which resulted in an outlier point for selected spectral bands (Fig. 6-1d) on LSERs for those dyes, may also manifest themselves in the region of the LSER that corresponds to  $\bar{\nu}_{\max}$  for linear alkane solvents ( $\pi^* \leq 0.00$ ). Our previous argument that the -decyl and -dodecyl chains become part of the solvent in the region of the *n* orbital for DNAP indicators may explain the observed decrease in sensitivity of  $\Delta\bar{\nu}_{\max}$  as a function of solvent  $\pi^*$  in the 'alkane' region of the LSER. This phenomenon is best illustrated in the LSER for



**Table 5.** Values of  $-s$ , current and previous, for DNAP and 4-alkoxynitrobenzenes

Indicator	Method of $\lambda_{\max}$ fit	# solvents	$\bar{\nu}_0$	$-s$	References	
<b>1a</b> (dimethyl)	90%	7	28.18	3.445	Carrozzino <i>et al.</i> (2004) <sup>8</sup>	
	90%	7	28.23	3.464	Helburn <i>et al.</i> (1997) <sup>4</sup>	
	90%	28	28.10	3.436	Kamlet <i>et al.</i> (1977) <sup>1</sup>	
	90%	20	28.18	3.44	This work	
	Gaussian fit	20	28.17	3.384	This work	
	Lorentzian fit	20	28.17	3.386	This work	
<b>1b</b> (diethyl)	90%	7	27.52	3.130	Carrozzino <i>et al.</i> (2004) <sup>8</sup>	
	90%	7	27.52	3.136	Helburn <i>et al.</i> (1997) <sup>4</sup>	
	90%	28	27.52	3.182	Kamlet <i>et al.</i> (1977) <sup>1</sup>	
	90%	20	27.53	3.125	This work	
	Gaussian fit	20	27.55	3.145	This work	
	Lorentzian fit	20	27.55	3.146	This work	
<b>1c</b> (di-propyl)	90%	7	27.41	3.114	Carrozzino <i>et al.</i> (2004) <sup>8</sup>	
	90%	7	27.39	3.007	Helburn <i>et al.</i> (1997) <sup>4</sup>	
	90%	21	27.39	3.067	This work	
	Gaussian fit	21	27.43	3.067	This work	
	Lorentzian fit	21	27.43	3.07	This work	
	<b>1d</b> (di-octyl)	90%	7	27.18	2.921	Carrozzino <i>et al.</i> (2004) <sup>8</sup>
90%		20	27.30	2.971	This work	
Gaussian fit		20	27.30	2.906	This work	
Lorentzian fit		20	27.30	2.958	This work	
<b>1e</b> (di-decyl)		90%	7	27.21	2.956	Carrozzino <i>et al.</i> (2004) <sup>8</sup>
		90%	20	27.26	2.9608	This work
	Gaussian fit	20	27.25	2.927	This work	
	Lorentzian fit	20	27.25	2.928	This work	
	<b>1f</b> (di-dodecyl)	90%	20	27.32	2.997	This work
		Gaussian	20	27.33	3.017	This work
Lorentzian		20	27.35	3.04	This work	
<b>2a</b> (methoxy)		90%	28	34.17	2.410	Kamlet <i>et al.</i> (1977) <sup>1</sup>
		Gaussian	21	34.16	2.409	This work
		Lorentzian	21	34.16	2.405	This work
	<b>2b</b> (-octyloxy)	Gaussian	22	33.91	2.433	This work
		Lorentzian	22	33.91	2.425	This work
		<b>2c</b> (-decyloxy)	Gaussian	23	33.95	2.436
Lorentzian			23	33.95	2.415	This work

*N,N*-didodecyl-4-nitroaniline (Fig. 8). As the polarity of the solvent approaches that of a linear alkane ( $\pi^* < 0.00$ ), solute–solvent interactions which are fewer than those for the more dipolar solvents become dominated by the long alkyl chains on the indicator, which is now more alkyl-like than phenyl-like, such that the solvent in the region of the  $n$  electrons becomes essentially unchanging and unable to elicit any further shift in the dipolar nature of the probe molecule. The result is an overall decrease in sensitivity of  $\bar{\nu}_{\max}$  to changes in solvent  $\pi^*$  in the negative  $\pi^*$  region of the plot (Fig. 8). It is of interest to note that the organization of alkyl chains for DNAP indicators in the context of their crystal structure also is different for the short and long chain species. In a previous paper,<sup>5</sup> we reported that the layered packing of **1c** (*N,N*-dipropyl-4-nitroaniline) lacks a center of symmetry resulting in a polar crystal, while layers of *N,N*-didodecyl-4-nitroaniline (**1d**) exhibit cosymmetry such that the crystal is non-polar.<sup>5</sup>

The observed change in  $-s$  over the range of carbon-chain length illustrated for both DNAP and nitrophenyl ether indicators (Fig. 9) is in support of the

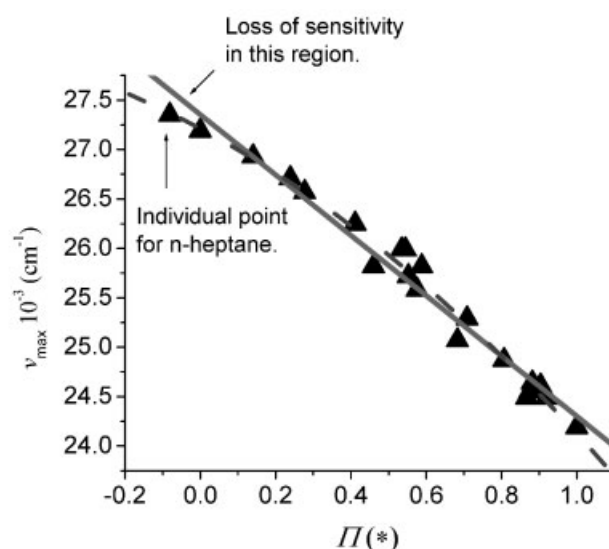


**Figure 8.** LSER ( $\nu_{\max}$  vs.  $\pi^*$ , Eqn. 1) for *N,N*-didodecyl-4-nitroaniline. Values of  $\bar{\nu}_{\max}$  determined by Lorentzian fitting of the upper portion of individual indicator bands. Linear fit (—)  $r^2 = 0.9730$ ; polynomial fit (---)  $r^2 = 0.9843$ ;

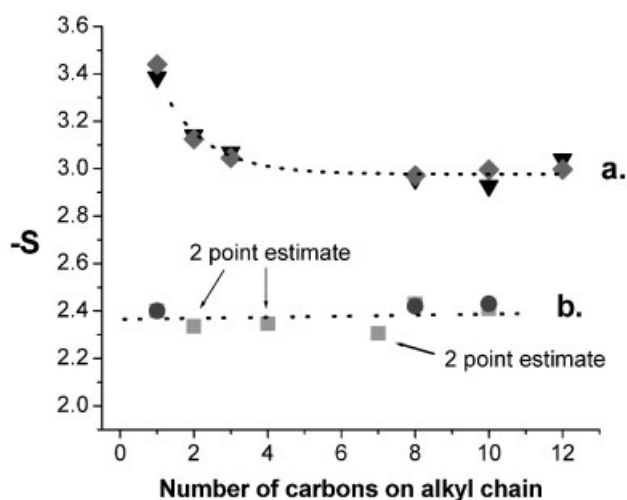


**Figure 9.**  $-s$  versus # of carbons on alkyl chain. (a) Plot for DNAP indicators including points obtained from  $\bar{\nu}_{\max}$  estimated via the 90% ( $\diamond$ ) and Lorentzian fit ( $\nabla$ ); plot is fitted with a 1st order exponential decay and (b) plot for 4-nitroalkoxybenzenes including points obtained from  $\bar{\nu}_{\max}$  estimated via Gaussian band fit ( $\square$ ) and Lorentzian band fit ( $\bullet$ ). Three center points ( $\square$ ) indicated by arrows represent two-point estimates of  $-s$  (based on  $\bar{\nu}_{\max}$  for cyclohexane and DMSO only) for the  $C_2$ ,  $C_4$ , and  $C_7$  4-alkyloxynitrobenzenes,<sup>18</sup> these points were added to confirm linearity of the plot

proposed mechanisms that we have discussed, though it should be emphasized that  $s(d\bar{\nu}_{\max}/d\pi^*)$  represents an average indicator response over many solvents rather than specific spectral details (such as we have discussed in the case of selected solvents). Overall,  $-s$  is larger for the DNAP indicators than for the nitrophenyl ether dyes (Table 5) due, at least in part, to the stronger electron-donating properties of the  $-NR_2$  dialkylamino substituent over that of the  $-OR$  alkyloxy group, which when paired with an electron-accepting  $-NO_2$  through the conjugated system (Fig. 3), results in a stronger intramolecular dipole (for DNAP) that is better aligned with the solvent dipole, especially for the excited state (Fig. 3e).<sup>17</sup> Thus  $d\Delta E_T/d\pi^*$ , which is directly proportional to  $-s$ , is larger and more pronounced for DNAP indicators than for the alkyloxy dyes, with a slightly larger range of spectral shift positions for the former. However, in the case of the DNAP indicators, these effects vary with alkyl chain length (Fig. 9a). The decrease in  $-s$  on moving from dimethyl (**1a**) to diethyl (**1b**) and the dipropyl (**1c**) indicators can be explained by the corresponding increase in shielding of the lone  $n$  electrons by the increasing bulk and motions of the alkyl groups, an effect that levels off with further increase in carbon number, forming a trend that is best illustrated by a 1st order decay (Fig. 9a). The orientation of the lone pair with respect to the two alkyl chains, the neighboring  $\pi^*$  orbital, and the solvent for the DNAP indicator (Fig. 1) is significantly different from

that of the lone pair on the alkyloxy dye (Fig. 2). The latter is more evenly exposed to the solvent over a wide range of alkyl chain lengths on the OR substituent. As a result,  $-s$  for the latter alkyloxy suite is essentially constant and linear over the range of methoxy, octyloxy, and decyloxy species (Fig. 9b). Note that we have inserted some two-point determinations of  $-s$ , based on  $\bar{\nu}_{\max}$  for indicators in DMSO and cyclohexane only, for the  $C_2$ ,  $C_4$ , and  $C_7$  alkyloxy indicators to confirm the linearity of the plot (Fig. 9b).

### Hydrophobic $\pi^*$ indicators, past and current effort

In an earlier paper of this type,<sup>4</sup> we made a strong argument for the  $N,N$ -dialkyl-4-nitroanilines as candidate structures for more hydrophobic versions of the  $\pi^*$  indicators<sup>1</sup> based on their relatively large values of  $-s$  and observed constancy of  $-s$  among some of the longer alkyl chain probes.<sup>4</sup> However, an equally strong argument can be made for the 4-alkyloxy nitrobenzenes on the basis of their 'less perturbing' single alkyl chain structure, more constant bandshape, and the constancy of  $-s$  over the entire range of carbon-chain lengths. While the phenylether dyes are slightly less sensitive to solvent dipolarity, that is,  $-s$  is smaller overall, this drawback may be more than compensated by a spectroscopic behavior that is stable over a wide range of solvent dipolarities and probe alkyl chain lengths. We note that intercalation of probes into lipid bilayers (a proposed application) may favor a more slender single alkyl chain shape over the more bulky dialkyl configuration. Overall, caution must be taken for all  $\pi^*$  indicators in over extending the length of alkyl chains such that gains made in generating hydrophobic character for the molecule are not compromised by a loss in their fundamental solvatochromic properties.

### REFERENCES

1. Kamlet MJ, Abboud J-LM, Taft RW. *J. Am. Chem. Soc.* 1977; **99**: 6027–6038.
2. Laurence C, Nicolet P, Tawfik-Dalati M, Abboud J-LM, Notario R. *J. Phys. Chem.* 1994; **98**: 5807–5816.
3. Taft RW, Abboud J-LM, Kamlet M. *J. Am. Chem. Soc.* 1981; **103**: 1080–1086.
4. Helburn R, Ullah N, Mansour G, Maxka J. *J. Phys. Org. Chem.* 1997; **10**: 42–48.
5. Mansour G, Creedon W, Dorrestein PC, Maxka J, Macdonald JC, Helburn R. *J. Org. Chem.* 2001; **66**: 4050–4054.
6. Helburn R, Dijiba Y, Mansour G, Maxka J. *Langmuir* 1998; **14**: 7147–7154.
7. Vitha MF, Weckwerth JD, Odland K, Dema V, Carr P. *J. Phys. Chem.* 1996; **100**: 18823–18828.
8. Carrozzino JM, Fuguet E, Helburn R, Khaledi M. *J. Biochem. Biophys. Methods* 2004; **60**(2): 97–115.
9. Lu H, Rutan SC. *Anal. Chem.* 1996; **68**(8): 1387–1393.
10. Helburn R, Rutan SC, Pompano J, Mitchem D, Patterson WT. *Anal. Chem.* 1994; **66**: 610–618.

11. Shin DM, Schanze KS, Otruba JP, Brown PE, Whitten DG. *Isr. J. Chem.* 1987/88; **28**: 37–45.
12. Nicolet P, Laurence C. *J. Chem Soc. Perkin Trans. 11* 1986; 1071–1079.
13. Creedon W. *MS Thesis, Northern Arizona University, USA, 1999.*
14. Compton D, Maxka J, Helburn R. *4th Annual Meeting of the Arizona-Nevada Academy of Science. Glendale, AZ, 1998.*
15. Allen CFH, Gates JW, Jr. *Org. Synth. Coll.* 1955; **3**: 140–141.
16.  $\lambda_{\text{max}}$  is taken as the midpoint between wavelengths corresponding to 90% of the maximum absorbance of the solvatochromic band [1].
17. Nitroaromatic  $\pi^*$  indicators exhibit 'positive' solvatochromism, i.e. spectral bands shift to longer wavelengths with increasing solvent dipolarity, implying that the excited state of the dye is more dipolar (in response to solvation) than the ground state.
18. C<sub>2</sub>, C<sub>4</sub>, and C<sub>7</sub> alkyl-4-nitrophenyl ethers were synthesized using methods as described. Only the longest alkyl chain species (C<sub>8</sub> and C<sub>10</sub>) were fully characterized in 23 non-HBD solvents.